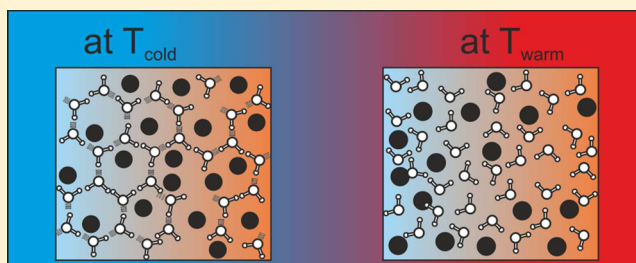


# Thermal Diffusion of Nucleotides

Zilin Wang,\* Hartmut Kriegs, and Simone Wiegand\*

ICS-Soft Condensed Matter, Forschungszentrum Jülich GmbH, D-52428 Jülich, Germany

**ABSTRACT:** We investigate the thermal diffusion behavior of aqueous solutions of nucleotides using an infrared thermal diffusion forced Rayleigh scattering (IR-TDFRS) setup. In this work we study 5 nucleotides: cyclic nucleotides adenosine and guanosine monophosphate, 5'-adenosine and 5'-cytidine monophosphate, and also adenosine diphosphate in water. The structures of nucleotides vary systematically, which results in different physical properties such as acidity, solubility, hydrophobicity, and melting point. We discuss the connection between the thermal diffusion behavior and the properties of the different nucleotides. Additionally, as in the case of the alkanes and monosaccharides, we find a correlation between the thermal diffusion coefficient and the ratio of the thermal expansion coefficient and the kinematic viscosity.



## INTRODUCTION

Thermal diffusion, i.e., the mass transport caused by a temperature gradient, influences many processes in multi-component systems. Lately, the effect has been used in the analysis of protein interactions.<sup>1</sup> But it is also used in polymer analysis and plays an important role in the distribution of crude oil components in geological fields. Recent simulations suggest that nucleotides and nucleic acid oligomers can be concentrated in prebiotic deep-sea alkaline vents by means of the thermal gradients originated between the warm volcanic rock and cold ocean water.<sup>2</sup> Further, it has experimentally been demonstrated that protocells like vesicles can be concentrated in narrow channels with a thermogravitational configuration;<sup>3</sup> i.e., the thermal gradient is applied perpendicular to the gravity field into a vertical narrow cavity. A microthermal focusing field flow fractionation technique has been used to separate different bacteria.<sup>4</sup> Braun and co-workers found that DNA molecules can be trapped by means of thermal diffusion<sup>5</sup> and that DNA self-replicates in a temperature gradient.<sup>6</sup> An all-optical microfluidic fluorescence method has been used to determine the thermal diffusion properties of DNA.<sup>7,8</sup>

For many biological and synthetic systems the influence of charge by varying salt concentration or pH has been experimentally studied<sup>9–12</sup> and theoretically analyzed.<sup>13–15</sup> For all systems studied so far an increase of the Soret coefficient,  $S_T$ , with increasing Debye length,  $\lambda_{DH}$ , has been found. Although there has been a lot of research activities on aqueous synthetic and biological systems, there are still many open questions.

We still lack a microscopic description which relates shape, size, charge and hydration shell of the molecules to the thermal diffusion properties of aqueous systems, in a similar way as it has been done for alkane.<sup>16</sup> First systematic studies on the thermal diffusion behavior of aqueous systems have been performed for aqueous solutions of mono- and oligosaccharides.<sup>17,18</sup> Some important results for the monosaccharides are

that the thermal diffusion coefficient,  $D_T$ , increases linearly with the ratio of the thermal expansion coefficient and the kinematic viscosity,<sup>17</sup> and  $D_T$  decreases with increasing sugar length and approaches a plateau value.<sup>18</sup>

Although empirical correlations between the thermal diffusion properties of nonpolar organic mixtures and the structure and size of the constituents are known,<sup>16,19,20</sup> those concepts fail for aqueous mixtures. The only correlation, which has been found also for some aqueous mixtures is the linear dependence of  $D_T$  on the ratio of the thermal expansion coefficient and the viscosity. Moreover, a universal temperature dependence of the Soret coefficient has been found for many aqueous systems<sup>9,21</sup> except for poly(*N*-isopropylacrylamide) in water. For many system the temperature dependence of the Soret coefficient can be described by an empirical law,<sup>9</sup>

$$S_T(T) = S_T^\infty \left[ 1 - \exp\left(\frac{T^* - T}{T_0}\right) \right] \quad (1)$$

with the parameters  $S_T^\infty$ ,  $T^*$ , and  $T_0$ .

We assume that the physical mechanism behind this universal temperature dependence of  $S_T$  is related to the formation of hydrogen bonds in aqueous solutions. In order to gain better intuitive feeling for this observation, we try to adopt a free energy minimization concept, which is often used to explain the closed loop phase diagrams under isothermal conditions to this nonisothermal condition. Strictly speaking, a free energy is not defined under nonisothermal conditions. However, experimental and theoretical studies have shown that local thermodynamic equilibrium can be successfully applied to describe thermophoresis.<sup>22,23</sup> As illustrated in Figure 1a, the system can locally minimize its free energy  $F = U - TS$  by the

Received: April 5, 2012

Revised: May 22, 2012

Published: June 4, 2012

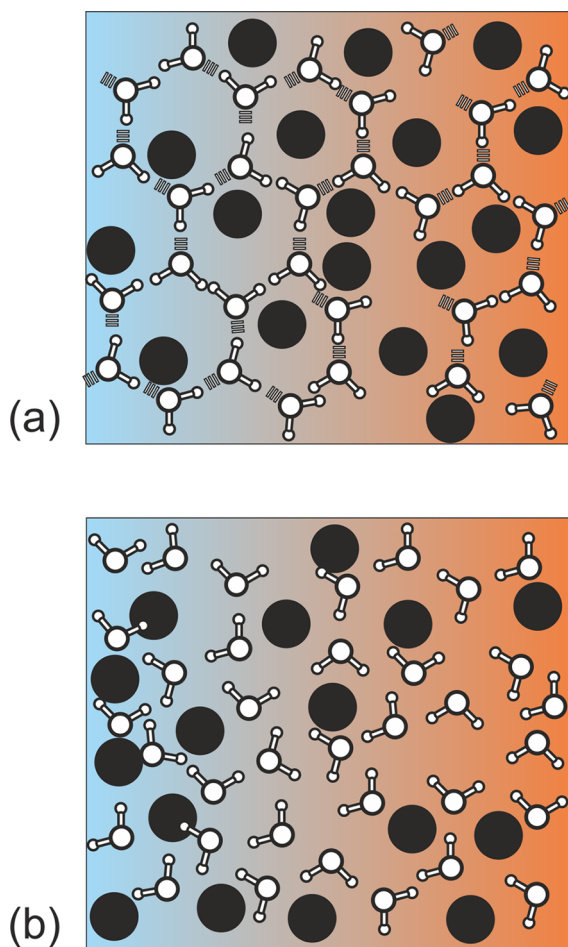


**Figure 1.** (a) At low overall temperatures the system reduces inner energy by forming hydrogen bonds on the cold side. (b) At higher overall temperatures, the system minimizes free energy by increasing the translational and orientational entropy.

formation of hydrogen bonds, so that at lower overall temperature the water molecules accumulate on the cold side and the solute molecules on the warm side. At high overall temperatures the energy gain due to the formation of hydrogen bonds becomes less important, therefore the system minimizes its free energy by maximizing the orientational entropy as illustrated in Figure 1b. Thus, it is favorable for the small water molecules to be on the warm side in order to maximize their orientational and translational entropy. The influence of hydrogen bonds on the thermodynamic properties has also been used to explain sign changes of the thermophoretic motion in aqueous solutions and binary mixtures.<sup>24,25</sup> In these studies, a direct correlation between the breakdown of the hydrogen bond network and the sign change concentration has been observed.

Studying the thermal diffusion behavior of nucleotides, which are the building blocks of DNA and RNA is another important step toward a better understanding of biological systems and to validate the hypothesis that thermal gradients are essential for the origin of life. On the basis of the phosphorylated nucleoside structure, the conformation of nucleotides can be varied by the chain length of phosphate and the type of bases. The study of nucleotides in aqueous solution is of particular interest since it offers the possibility to tune the number of charges on the molecules<sup>26</sup> or the base ring-phosphate interactions by

changing the pH value.<sup>27</sup> NMR studies show that a decreasing pH, which causes deprotonation of phosphate, increases the probability for the *anti* conformation of 5'-adenosine monophosphate (AMP). On the other hand, a temperature change also affects the conformation.<sup>27,28</sup> Unfortunately, the nucleotides cannot not be modified so systematically in their shape variation, and the variety of the nucleotides is much larger compared to the saccharides. An additional important aspect for the investigation of nucleotides is the presence of charges, so that we can study charge effects on a low molecular weight level, which will also influence the thermal diffusion behavior of large biomolecules such as DNA and proteins.

In this work we investigate the thermal diffusion phenomena of cyclic nucleotides adenosine and guanosine monophosphate (cAMP and cGMP), 5'-adenosine and 5'-cytidine monophosphate (AMP and GMP) and also adenosine diphosphate (ADP) in water. For all five systems we perform temperature and pH dependent measurements of the thermal diffusion properties with the infrared thermal diffusion forced Rayleigh setup (IR-TDFRS). Additionally, we perform also temperature dependent density measurements to examine the correlation between the thermal diffusion coefficient and the ratio of the thermal expansion coefficient and the viscosity. The structures are shown in Figure 2.

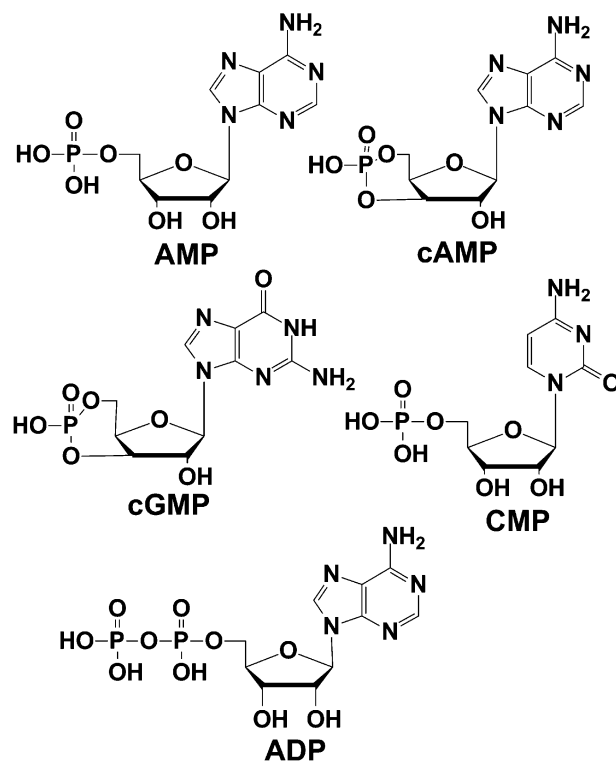


**Figure 2.** Structure of investigated nucleotides.

## EXPERIMENTAL SECTION

**Sample Preparation and Characterization.** cAMP ( $\geq 98.5\%$ ), AMP ( $\geq 97\%$ ), cGMP ( $\geq 98\%$ ), ADP ( $\geq 95\%$ ), and CMP ( $\geq 99\%$ ) were purchased from Sigma-Aldrich and were used without further purification. Deionized water from a Millipore filter unit ( $0.22\ \mu\text{m}$ ) was used to prepare all aqueous solutions.

Approximately 2 mL of the prepared solutions were filtered through a 0.2  $\mu\text{m}$  filter (Whatman Anotop 10) before filling them into an optical quartz cell (Hellma) with an optical path length of 0.2 mm. At least two measurements with different cells and freshly prepared samples were done for each system.

The refractive index increments with the mass concentration  $(\partial n/\partial c)_{p,T}$  was measured by an Anton Paar RXA 156 refractometer, whose accuracy is 0.00002 nD with a temperature control of  $\Delta T = \pm 0.03\text{K}$ . For each nucleotide, the refractive index has been measured for at least three concentrations around the desired concentration. The slope of the linear interpolation of the refractive index as a function of the concentration gives  $(\partial n/\partial c)_{p,T}$ . The refractive index increments with temperature  $(\partial n/\partial T)_{p,c}$  was measured interferometrically,<sup>29</sup> in a temperature range of 1 K around the temperature of interest. The refractive index varied linearly with temperature and concentration in the investigated range. The refractometer uses the sodium line with a wavelength of 589.3 nm, which is roughly 40 nm shorter than the HeNe-laser of 632.8 nm used as read-out beam in the IR-TDFRS. This causes a small systematic error in the refractive index increment in the order of 0.5–1%.<sup>30,31</sup>

All measurements are performed in the temperature range of 30 and 70  $^{\circ}\text{C}$ , since below 30  $^{\circ}\text{C}$  the solubility of the nucleotides is too low to get a good signal and above 70  $^{\circ}\text{C}$  the nucleotides start to decompose.

**Infrared Thermal Diffusion Forced Rayleigh Scattering.** A detailed description of the recently modified IR-TDFRS can be found in the paper by Blanco et al.<sup>12</sup> This setup is optimized for aqueous systems and has been used to study the transport properties in different aqueous systems of nonionic surfactants,<sup>32,33</sup> saccharide solutions<sup>17,18</sup> and anisotropic biocolloids.<sup>12</sup>

The normalized heterodyne scattering intensity  $\zeta_{\text{het}}(t)$ , assuming an ideal excitation with a step function, is given by

$$\zeta_{\text{het}}(t) = 1 - \exp\left(-\frac{t}{\tau_{\text{th}}}\right) - A(\tau - \tau_{\text{th}})^{-1} \left\{ \tau \left[ 1 - \exp\left(-\frac{t}{\tau}\right) \right] - \tau_{\text{th}} \left[ 1 - \exp\left(-\frac{t}{\tau_{\text{th}}}\right) \right] \right\} \quad (2)$$

with the steady state amplitude  $A$

$$A = \left(\frac{\partial n}{\partial c}\right)_{p,T} \left(\frac{\partial n}{\partial T}\right)_{p,c}^{-1} S_T c(1 - c) \quad (3)$$

where  $c$  is the mass fraction,  $\tau_{\text{th}}$  the heat diffusion time, and  $(\partial n/\partial c)_{p,T}$  and  $(\partial n/\partial T)_{p,c}$  are refractive index contrast factors with respect to mass concentration at constant pressure and temperature and referring to temperature at constant pressure and mass concentration, respectively. The equilibration time for the temperature grating  $\tau_{\text{th}}$  can be used to calculate the thermal diffusivity,  $D_{\text{th}}$ , which describes the heat transport in the solution. It is related to the thermal conductivity,  $\kappa$ , specific heat capacity,  $c_p$  and density,  $\rho$  by

$$D_{\text{th}} = \frac{\kappa}{\rho c_p} \quad (4)$$

The Soret coefficient,  $S_T = D_T/D$ , can be expressed as ratio of the thermal diffusion coefficient,  $D_T$ , and the collective diffusion coefficient,  $D$ . Whereas the diffusion coefficient  $D = 1/(q^2\tau)$

can be calculated from the diffusion time,  $\tau$  (cf. eq 2), using the magnitude of the grating vector  $q$ , which is given by  $q = (4\pi)/\lambda_w \sin(\theta/2)$ . Here  $\theta$  is the angle between the two writing beams and  $\lambda_w$  is the wavelength of the laser beam. The transport coefficients are determined by fitting eq 2 to the measured heterodyne signal and deconvoluting the excitation function.<sup>34,35</sup>

Figure 3 shows the normalized heterodyne signals of only 100 mM TRIS buffer and of cAMP (wt = 0.5%) in 100 mM

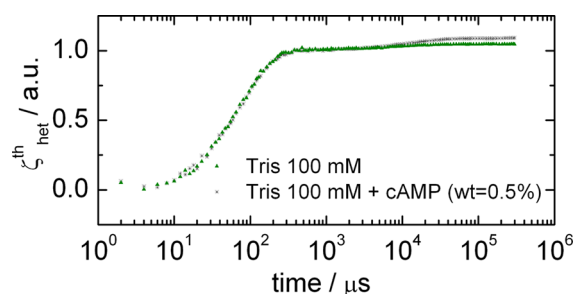


**Figure 3.** Normalized heterodyne signal  $\zeta_{\text{het}}^{\text{th}}$  of TDFRS measurements for 100 mM TRIS buffer and a solution of cAMP (wt = 0.5%) in 100 mM TRIS buffer.

TRIS buffer. It is obvious that the buffer solution itself contributes to the concentration part of the heterodyne signal. This leads to some uncertainty in the data analysis of the nucleotides in buffer solutions, which makes it difficult to draw significant conclusions. Therefore, we decided to perform all measurements in pure water, which leads to more reliable results. This shows that reproducible measurements of the thermal diffusion behavior by methods, which rely on refractive index contrast, become difficult, if biomolecules are dissolved in buffer or nutrient solutions. In these cases, often methods using fluorescent labeling are superior, but the investigation of nucleotides by fluorescent methods is also a difficult task, because the typical fluorescent marker are comparable in mass and size and will influence the transport properties of the nucleotides. Also methods such as thermogravitational columns, which can handle multicomponent solutions, are not feasible due to fairly large sample volumes in the order of typically 20 mL and the high costs of the nucleotides.

## RESULTS AND DISCUSSION

First of all, we discuss the temperature dependence of  $S_T$ ,  $D$ , and  $D_T$  for aqueous solutions of various nucleotides, which are shown in Figure 4 in the investigated temperature range. Both diffusion coefficients  $D$  and  $D_T$  increase with temperature. This indicates that nucleotides diffuse faster at higher temperature, which is related to the decreasing viscosity of water with increasing temperature.  $S_T$ , which describes the separation between the nucleotide and water, at first glance shows a weaker temperature dependence compared to DNA and other biomolecules. But actually this is a matter of the regarded temperature range. Looking at the overall trend of the temperature dependence of  $S_T$  expressed by eq 1, we find for higher temperatures in general a weaker temperature dependence. As shown in Figure 5,  $S_T$  of DNA (6.7 kbp) and one of the nucleotides CMP are both normalized to  $S_T(30\text{ }^{\circ}\text{C})$ . Although we have only two measured temperatures, which overlap with the temperature range of DNA measurement, it is possible to extrapolate the fitted curve in the high temperature

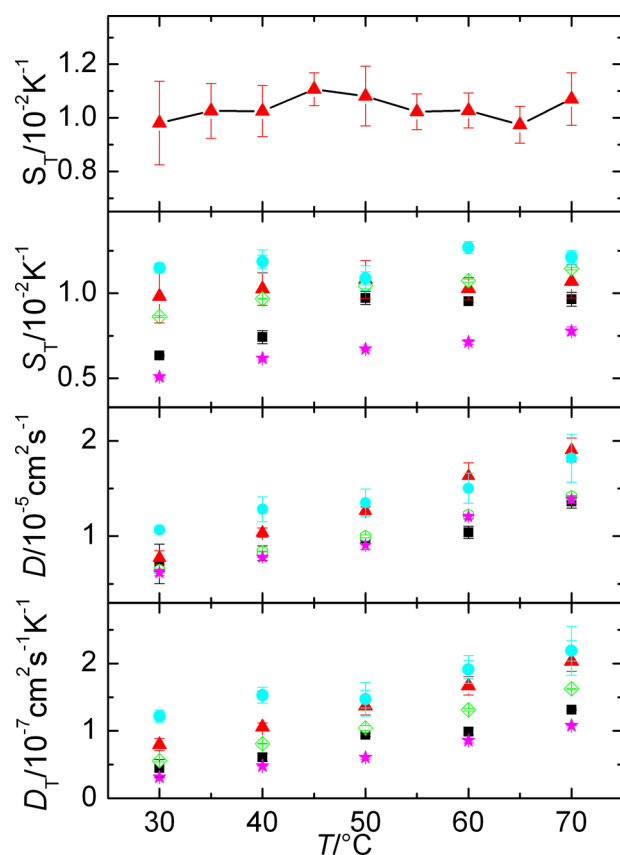


**Figure 4.**  $S_T$ ,  $D$ , and  $D_T$  for CMP (pink star), AMP (black box), cAMP (green diamond), cGMP (red triangle) and ADP (blue circle) with a concentration of 0.5 wt % in water.  $S_T$  of cGMP is plotted separately with a better temperature resolution. The solid line is the guide to the eye. The error bars correspond to the standard deviation of repeated measurements. Because of the absence of a buffer solution the pH was around 2.

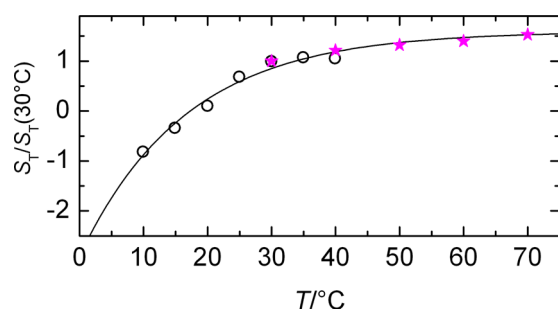


**Figure 5.**  $S_T$  of DNA (black ring) fitted by eq 1. Data are obtained by digitizing figures of original paper.<sup>9</sup>  $S_T$  of CMP (pink star) is also shown as comparison. All the  $S_T$  are normalized at 30 °C.

regime by fitting only the DNA data with eq 1. As expected,  $S_T$  of DNA increases rapidly with temperature in the cold regime, while in the high temperature regime, it shows a temperature dependence as weak as for the nucleotides. The absence of the buffer solution can lead to a change of the pH value with increasing temperature. However, the nucleotides contain both phosphate and amino groups, which release positive or negative charges, respectively. This helps to balance the pH value. The pH values of different nucleotide solutions differ slightly due to the presence of different chemical groups. The pH value of AMP and CMP solutions is around 2.6, slightly higher than the

values for the other nucleotide solutions, which are 2.2 for cAMP and 1.6 for cGMP and ADP. We measured the temperature dependence of the pH value for cAMP and CMP, exemplary. The pH value declines 0.02 and 0.05 units for cAMP and CMP, respectively, when the temperature is raised by 10 K. This pH change enhances the temperature effect of  $S_T$ , which could explain the stronger temperature dependence of CMP and AMP compared to the other nucleotides.

For many systems the Soret coefficient increases steadily with temperature. In contrast, some of the nucleotides show a “dip” in  $S_T$  at temperatures around 60 °C, specifically ADP and cGMP. According to earlier publications by Son et al.<sup>28</sup> and Wang et al.,<sup>27</sup> NMR studies indicated that there is a conformational change between *syn* and *anti* conformers. In order to quantify this we performed NMR and microcalorimetry measurements in the relevant temperature range. None of our results are conclusive enough to confirm this conformational change. This might indicate that the energy difference between the two conformational statuses is below  $kT$ , so that both conformations are occupied and no clear transition can be observed.

Additionally, we analyze also the thermal diffusivity,  $D_{th}$ , and calculate the specific heat capacity,  $C_p$ , according to eq 4, whereas we use the value of thermal conductivity of pure water and the measured density of the nucleotide solutions. The measured  $D_{th}$  and calculated  $C_p$  are shown in Figure 6, parts a and b, respectively.  $D_{th}$  of all nucleotides increase linearly with temperature, but the heat capacity of the nucleotides shows no clear monotonic trend, which is however not correlated with the variation of  $S_T$ . In comparison, water does not show any

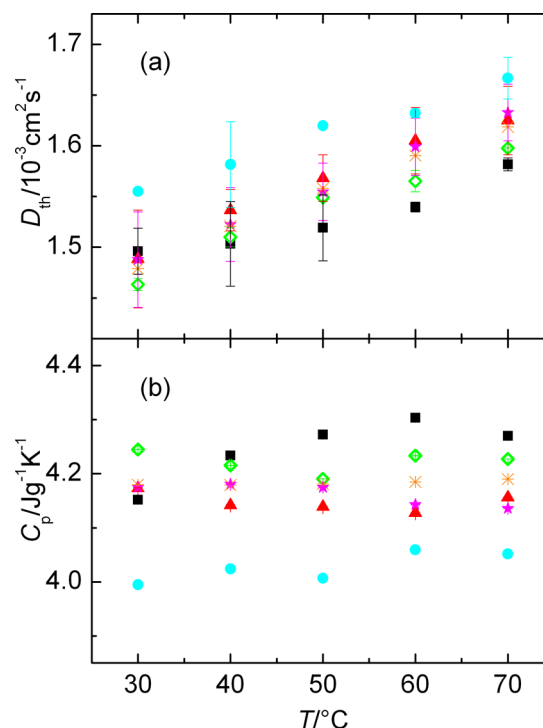


**Figure 6.** Measured thermal diffusivity and calculated heat capacity of nucleotides as a function of temperature. Thermal conductivity of water<sup>37</sup> was used to calculate the heat capacity. For nucleotides we used the same symbols as in Figure 4. For comparison, we added water (brown asterisk). Error bars are included in both thermal diffusivity and heat capacity and are too small to be seen in the latter case.



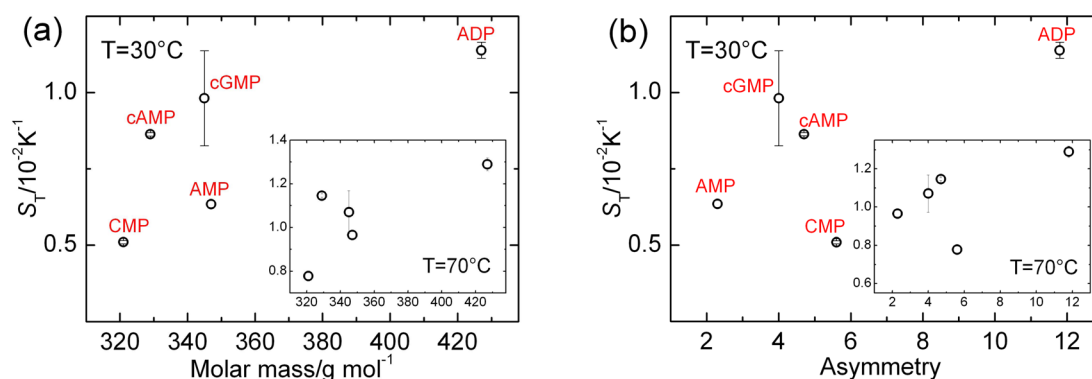


**Figure 7.** Soret coefficient of nucleotides in water with a weight fraction  $c = 0.5\%$  at  $T = 30$  and  $70^\circ\text{C}$  as a function of (a) mass and (b) asymmetry of the molecules, defined by ratio of the principle moments of inertia. For further details, see the text.

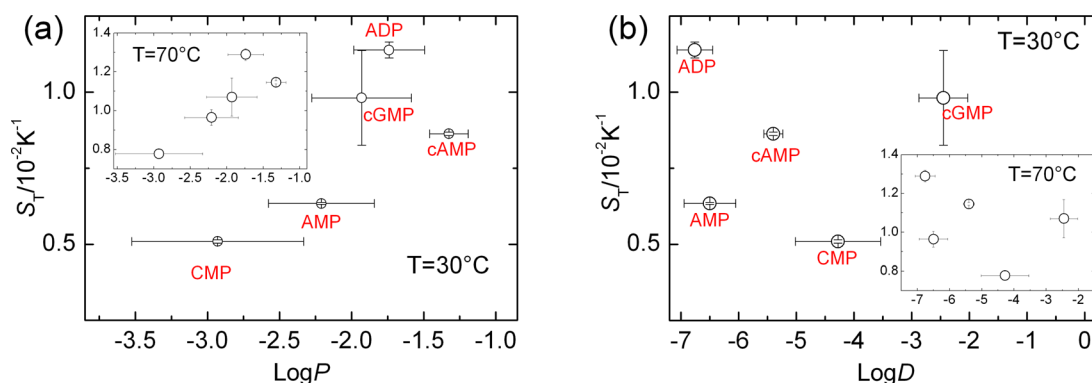


**Figure 8.** Soret coefficient of nucleotides in water with a weight fraction  $c = 0.5\%$  at  $T = 30$  and  $70^\circ\text{C}$  as a function of (a)  $\log p$ , partition coefficient, (b)  $\log d$ , distribution coefficient.

temperature dependence in the investigated temperature range. None of the thermophysical properties confirm our hypothesis of the conformational change. This is in contrast with the measurements by Braun's group, who found a clear signature in the thermal diffusion behavior, when a conformational change for proteins occurred.<sup>36</sup>

The next question we raised is, whether there is a correlation between the structure of the nucleotides and their thermophysical properties. There are several examples in the literature, where a correlation between structure and thermal diffusion behavior has been observed, but preferentially for nonpolar systems.<sup>16,38</sup> In order to investigate whether the measured  $S_T$  relates with the mass or symmetry of the nucleotides, we plotted Soret coefficients as a function of mass and asymmetry at 30 and  $70^\circ\text{C}$  in Figure 7, parts a and b. Here, asymmetry is defined as the ratio of the principle moments of inertia of  $x$ -direction and  $z$ -direction, which are calculated by an atomistic model for single molecules in vacuum.<sup>39</sup> The Soret coefficients show no clear correlation with mass and asymmetry. Only the heaviest and most asymmetric nucleotide ADP always stays at the top.

Former studies showed that formation of hydrogen bond plays a very important role in aqueous system.<sup>24</sup> Therefore, we tried to find a criterion, which describes the hydrophobicity of the nucleotides. One concept often used for drug compounds is the partition coefficient,  $P$  and the distribution coefficient  $D$ , which are defined as the ratio of concentrations of a compound dissolved in the two phases of a mixture of water and organic solvent at equilibrium. The most commonly used organic solvent is octanol. The partition coefficient consists of the

concentrations of the un-ionized solute, while the calculation of distribution coefficient contains also the ionized solute concentration of water and is pH dependent. The logarithmic expressions  $\log p = \log([\text{solute}]_{\text{octanol}})/([\text{solute}]_{\text{water}}^{\text{un-ionized}})$  and  $\log d = \log([\text{solute}]_{\text{octanol}})/([\text{solute}]_{\text{water}}^{\text{ionized}} + [\text{solute}]_{\text{water}}^{\text{neutral}})$  are often used to quantify the hydrophobicity of a compound. Positive  $\log p$  and  $\log d$  values are found for hydrophobic compounds, while negative values are observed for hydrophilic substances. The partition coefficients of nucleotides can be calculated by adding the contributions of the different chemical groups present in the molecule.<sup>40</sup> The calculation of the distribution coefficient,  $\log d$ , includes further terms depending on the ionization at different pH value. On the basis of literature values<sup>41,42</sup> the obtained  $\log p$  and  $\log d$  values differ considerably, which leads to fairly large error bars. Figure 8a displays that  $S_T$  shows an increasing trend with an increasing  $\log p$  value, which means that  $S_T$  becomes larger, when the nucleotide is more hydrophobic and is thus less soluble in water. We expect that  $\log d$  should be the better coefficient to describe the behavior of the nucleotides due to the ionization of water. However,  $\log d$  values show no correlation with Soret coefficients. A possible reason could be that the calculation of the pH value based on the dissociation constant of individual chemical groups is not sufficient to describe the experimental situation.

In order to investigate the charge influence we performed additional measurements at pH 5.2 and 10.2 with cAMP. As shown in Figure 9, for all pH values the coefficients increase with increasing temperature.  $S_T$  shows a strong pH dependence, while the collective diffusion coefficient has almost no pH

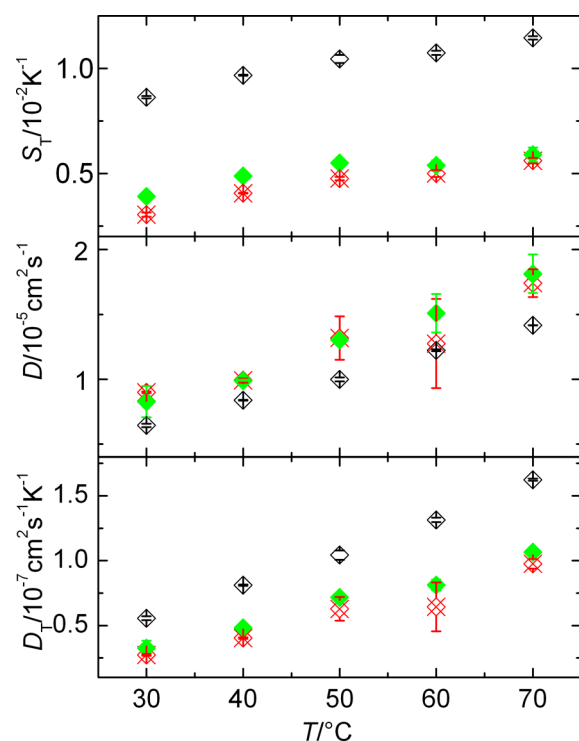


**Figure 9.**  $S_T$ ,  $D$ , and  $D_T$  for cAMP at pH 2.2 (black diamond), pH 5.2 (green diamond), and pH 10.2 (red crossed diamond) as a function of temperature.

dependence. At pH 2.2, the protonation of the amino group from the base should be more than the deprotonation of the phosphate group. At pH 5.2, which is the isoelectric point of cAMP, the molecules have the same amount of positive and negative charge.  $S_T$  increases rapidly from pH 2.2 to 5.2, but only slightly from 5.2 to 10.2. This is due to the definition of pH value. Also the ionic strength shows a much weaker pH-dependence at high pH values compared to low pH, which results in a linear dependence of the Soret coefficient on the ionic strength. Also the ammonium hydroxide added to adjust the pH value increases the ionic strength of the solution, which means a decline of the Debye length. This effect, that  $S_T$  increases with Debye length, has already been observed by Ning et al.<sup>10</sup> and Blanco et al.<sup>12</sup> with Ludox colloidal particles and fd-virus, respectively.

The last point we want to study in this work is the correlation between  $D_T$  and the thermal expansion coefficient  $\alpha$ . Brenner derived the expression  $D_T \propto \alpha D$  in his elementary theory of thermal diffusion. As  $D$  is inversely proportional to the kinematic viscosity  $\nu$ , we can deduce that  $D_T$  is proportional to  $\alpha/\nu$ . As indicated in Figure 10 for all the nucleotides, a linear dependence of  $D_T$  on the ratio of the thermal expansion coefficient  $\alpha$ , and the kinematic viscosity  $\nu$  is found. In this case, we use  $\alpha$  and  $\nu$  of water. This is justified because our solutions are very dilute. For the same  $\alpha/\nu$  of nucleotides, ADP, which has the largest hydrophobicity, has the strongest tendency to go to the cold side, while CMP is at the other end. The same linear  $\alpha/\nu$  dependence has already been observed for diluted aqueous monosaccharides solutions, but not for concentrated solutions.<sup>17</sup> This correlation is often found if one stays in one system class, as long as the system is isotropic and no phase changes occur. Therefore, this simple correlation is not valid for micellar systems.<sup>43</sup>

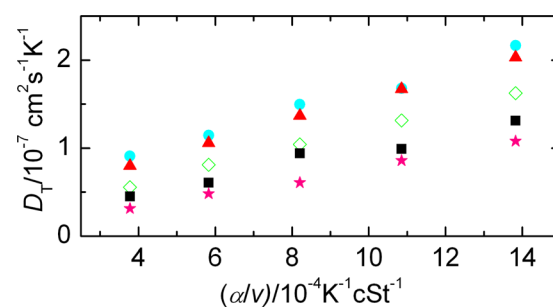


**Figure 10.**  $D_T$  of nucleotides as a function of the ratio of the thermal expansion coefficient,  $\alpha$ , and the kinematic viscosity,  $\nu$ . All the symbols are consistent with Figure 4.

## CONCLUSION

In this work, thermal diffusion properties of aqueous solutions of nucleotides are presented at different temperatures. The Soret coefficients of the nucleotides increase with increasing temperature in the measured temperature range. The obtained Soret coefficients and their temperature dependence are comparable to large biomolecules, such as DNA. However, compared to other systems with a similar molar mass, like oligosaccharide, the thermal diffusion coefficients of the nucleotides are 1 order of magnitude larger. The diffusion coefficients remain in the same range, which shows that we do not have aggregation problems.

We find a correlation between the thermal diffusion properties and hydrophobicity represented by the partition coefficient,  $\log p$ . However, it is difficult to correlate the Soret coefficient to structure and mass. Furthermore, the pH value has a strong influence on the thermal diffusion behavior of nucleotides, and the results are comparable with those found for charged colloids.<sup>10,12</sup> Additionally, we also find that the thermal diffusion coefficient is proportional to the ratio of the thermal expansion coefficient and kinematic viscosity.

Further research is needed to investigate whether thermal diffusion coefficients of nucleotides are large enough to support an origin of life scenario in temperature gradients.

## AUTHOR INFORMATION

### Corresponding Author

\*E-mail: (Z.W.) zil.wang@fz-juelich.de; (S.W.) s.wiegand@fz-juelich.de.

### Notes

The authors declare no competing financial interest.

## ACKNOWLEDGMENTS

We appreciate many fruitful discussions with Dieter Braun and Pablo Blanco. We express our gratitude to Jan Dhont for his generous support. We thank Sabine Willbold for performing the NMR measurements and Doris Vollmer for her help with the micro calorimetry experiments. Financial support due to the Deutsche Forschungsgemeinschaft Grant Wi 1684 is gratefully acknowledged.

## REFERENCES

- (1) Wienken, C. J.; Baaske, P.; Rothbauer, U.; Braun, D.; Duhr, S. *Nat. Commun.* **2010**, *1*, 100.
- (2) Baaske, P.; Weinert, F. M.; Duhr, S.; Lemke, K. H.; Russell, M. J.; Braun, D. *Proc. Natl. Acad. Sci. U.S.A.* **2007**, *104*, 9346–9351.
- (3) Budin, I.; Bruckner, R. J.; Szostak, J. W. *J. Am. Chem. Soc.* **2009**, *131*, 9628–9629.

- (4) Kasparkova, V.; Halabalova, V.; Simek, L.; Ruzicka, J.; Janca, J. *J. Biochem. Biophys. Methods* **2007**, *70*, 685–687.
- (5) Braun, D.; Libchaber, A. *Phys. Rev. Lett.* **2002**, *89*, 188103.
- (6) Mast, C. B.; Braun, D. *Phys. Rev. Lett.* **2010**, *104*, 188102.
- (7) Duhr, S.; Arduini, S.; Braun, D. *Eur. Phys. J. E* **2004**, *15*, 277–286.
- (8) Duhr, S.; Braun, D. *Proc. Natl. Acad. Sci. U.S.A.* **2006**, *103*, 19678–19682.
- (9) Iacopini, S.; Rusconi, R.; Piazza, R. *Eur. Phys. J. E* **2006**, *19*, 59–67.
- (10) Ning, H.; Dhont, J. K. G.; Wiegand, S. *Langmuir* **2008**, *24*, 2426–2432.
- (11) Reineck, P.; Wienken, C. J.; Braun, D. *Electrophoresis* **2010**, *31*, 279–286.
- (12) Blanco, P.; Kriegs, H.; Lettinga, M. P.; Holmqvist, P.; Wiegand, S. *Biomacromolecules* **2011**, 1602–1609.
- (13) Dhont, J. K. G.; Wiegand, S.; Duhr, S.; Braun, D. *Langmuir* **2007**, *23*, 1674–1683.
- (14) Dhont, J. K. G.; Briels, W. J. *Eur. Phys. J. E* **2008**, *25*, 61–76.
- (15) Würger, A. *Langmuir* **2009**, *25*, 6696–6701.
- (16) Polyakov, P.; Luettmer-Strathmann, J.; Wiegand, S. *J. Phys. Chem. B* **2006**, *110*, 26215–26224.
- (17) Blanco, P.; Wiegand, S. *J. Phys. Chem. B* **2010**, *114*, 2807–2813.
- (18) Blanco, P.; Kriegs, H.; Arlt, B.; Wiegand, S. *J. Phys. Chem. B* **2010**, *114*, 10740–10747.
- (19) Blanco, P.; Bou-Ali, M. M.; Platten, J. K.; Urteaga, P.; Madariaga, J. A.; Santamaria, C. *J. Chem. Phys.* **2008**, *129*, 174504.
- (20) Wittko, G.; Köhler, W. *J. Chem. Phys.* **2005**, *123*, 014506.
- (21) Kishikawa, Y.; Wiegand, S.; Kita, R. *Biomacromolecules* **2010**, *11*, 740–747.
- (22) Duhr, S.; Braun, D. *Phys. Rev. Lett.* **2006**, 96.
- (23) Astumian, R. D. *Am. J. Phys.* **2006**, *74*, 683–688.
- (24) Kita, R.; Wiegand, S.; Luettmer-Strathmann, J. *J. Chem. Phys.* **2004**, *121*, 3874–3885.
- (25) Ning, H.; Wiegand, S. *J. Chem. Phys.* **2006**, *125*, 221102.
- (26) Saenger, W. *Principles of nucleic acid structure*; Springer: New York, 1984.
- (27) Wang, P. M.; Izatt, R. M.; Oscarson, J. L.; Gillespie, S. E. *J. Phys. Chem.* **1996**, *100*, 9556–9560.
- (28) Guschlbauer, W.; Son, T. D. *Nucleic Acids Res.* **1975**, *2*, 873–86.
- (29) Becker, A.; Köhler, W.; Müller, B. *Ber. Bunsen-Ges. Phys. Chem. Chem. Phys.* **1995**, *99*, 600–608.
- (30) Camerini-Otero, R. D.; Franklin, R. M.; Day, L. A. *Biochemistry* **1974**, *13*, 3763–3773.
- (31) Sechenyh, V. V.; Legros, J.; Shevtsova, V. *J. Chem. Thermodyn.* **2011**, *43*, 1700–1707.
- (32) Ning, H.; Datta, S.; Sottmann, T.; Wiegand, S. *J. Phys. Chem. B* **2008**, *112*, 10927–10934.
- (33) Arlt, B.; Datta, S.; Sottmann, T.; Wiegand, S. *J. Phys. Chem. B* **2010**, *114*, 2118–2123.
- (34) Wittko, G.; Köhler, W. *Philos. Mag.* **2003**, *83*, 1973–1987.
- (35) Ning, H.; Kita, R.; Kriegs, H.; Luettmer-Strathmann, J.; Wiegand, S. *J. Phys. Chem. B* **2006**, *110*, 10746–10756.
- (36) Wienken, C.; Baaske, P.; Duhr, S.; Braun, D. *Nucleic Acids Res.* **2011**, *39*, 1–10.
- (37) Kreith, F. *The CRC Handbook of Thermal Engineering*; CRC Press: Boca Raton, FL, 2000.
- (38) Köhler, W.; Debuschewitz, C. *Phys. Rev. Lett.* **2001**, *87*, 055901.
- (39) CambridgeSoft: Chem3d, V.12. 2010.
- (40) ChemAxon: Marvin 5.9.0. 2012.
- (41) Viswanadhan, V. N.; Ghose, A. K.; Revankar, G. R.; Robins, R. K. *J. Chem. Inf. Comput. Sci.* **1989**, *29*, 163–172.
- (42) Klopman, G.; Li, J.-Y.; Wang, S.; Dimayuga, M. *J. Chem. Inf. Comput. Sci.* **1994**, *34*, 752–781.
- (43) Arlt, B. Thermal diffusion in binary surfactant systems and microemulsions. Ph.D. Thesis, Universität zu Köln: Cologne, Germany, 2011.